# Collisionless absorption in clusters out of linear resonance

P. Mulser
*Theoretical Quantum Electronics (TQE), Technische Universität Darmstadt, Schossgartenstrasse 7, 64289, Darmstadt, Germany*

M. Kanapathipillai
*Institut für Kernphysik, Technische Universität Darmstadt, Schossgartenstrasse 7, 64289, Darmstadt, Germany*
*and Gesellschaft für Schwerionenforschung, Planckstrasse 1, D-64291 Darmstadt, Germany*
(Received 19 November 2004; published 7 June 2005)

So far all analytic models of heating of clusters in the collisionless domain are based on linear or linearized concepts, like Mie resonance or other linear oscillations. They are characterized by constant eigenfrequencies lying well above the frequencies of most intense lasers. In this paper we show that nonlinear resonant excitation constitutes the basis of absorption in the collisionless domain, for individual electrons as well as for entire electron bunches. With increasing amplitude of the particles oscillating in their own space charge field their eigenperiod increases and at sufficient driver strength it equals and exceeds the constant laser period. At the crossing point, and essentially only there, resonant absorption takes place. Neither nonlinearities in themselves nor asymmetric excitation of the electron cloud of the cluster leads to irreversible energy gain.

DOI: 10.1103/PhysRevA.71.063201 PACS number(s): 36.40.Gk, 52.50.Jm, 52.25.Os

## I. INTRODUCTION

High-power-laser interaction with atomic and metallic clusters of all kinds has gained increasing interest within the last decade. One of the prominent features of laser-cluster interaction is the strong coupling of the electromagnetic field to clustered matter at already moderate laser intensities of the order of $10^{16}$ W/cm$^2$. From Xe clusters highly stripped ions have been detected [1–3], in some cases up to the order $Z=40$ [4]. The excellent absorption of light brings the electron temperature up to several kiloelectron volts, and even more in some experiments [5]. The ion energies resulting from the concomitant cluster expansion ranged from several tens to about 100 keV. However, megaelectron volts ions of hitherto not well understood origin were also found [6,7]. Additional important experimental facts are the enhancement of emission of incoherent hard x rays [8–11] and higher harmonics of the laser frequency (coherent x rays) [12,13].

All experiments are conveniently done in media of under critical density on the average. In a homogeneous gas, under such conditions, the interaction of an intense laser beam is generally weak. On the other hand, the experimental facts mentioned above all indicate that there is a strong increase of laser light coupling when molecules or atoms cluster together [5]. The peculiar situation with clusters is that properties of solids mix up with the under-critical gas behavior: dielectric polarization effects are locally as high as in solids and light freely penetrates large regions since the gross optical behavior is not changed by clusters of dimensions much smaller than the laser wavelength. Various models have been developed along this line and some partial understanding of the increased coupling has been gained. For example, the enhanced field ionization in clusters relative to single atoms has been attributed to ionization ignition [14]. The efficient conversion into bremsstrahlung x rays and into short-wavelength $X$-line radiation is qualitatively understood from the better heating efficiency of the electrons and their interaction with more highly charged ions in clusters. A good overview on the state of the art in laser-cluster interactions is presented by review articles of Lezius and Schmidt, Tisch and Springate, and Smith and Ditmire [15].

The present understanding of laser absorption in clusters may be characterized as follows. In a first stage of irradiation the generation of free electrons by laser field ionization prevails [16] which, with increasing "outer" ionization may be reinforced and finally replaced by ionization in collective fields [14]. As the ionization process saturates, sometimes also named "inner ionization," heating of the plasma is due to electron-ion collisions, i.e., inverse bremsstrahlung. The typical electron temperatures $T_e$ observed in the kiloelectron volts domain, however, cannot be attributed to this absorption mechanism because already long before it quenches owing to the $T_e^{-3/2}$ and laser intensity $I_0^{-3/2}$ dependence of the electron-ion collision frequency $\nu_{ei}=\nu_{ei}(T_e,I_0)$. Rather, further absorption is due to collisionless collective effects [17]. Particle-in-cell (PIC) and molecular dynamics (MD) simulations by various research groups have proven absorption in the absence of electron-ion collisions to be very efficient in clusters [18–20]. Unfortunately computer simulations in general, and PIC calculations in particular, do not tell what the underlying physics is which leads to irreversibility. For this reason analytical models have to be developed to close this gap.

Under steady-state conditions all phenomena of absorption of intense laser light in extended media are described by the cycle-averaged Poynting theorem,

$$\overline{\nabla \cdot \boldsymbol{S}} = \overline{\boldsymbol{j} \cdot \boldsymbol{E}}, \tag{1}$$

where $I=|\boldsymbol{S}|$. When the electrons are free and their number is constant, as is the case for a homogeneous fully ionized plasma, a phase difference of $-\pi/2$ builds up between $\boldsymbol{j}$ and $\boldsymbol{E}$ and no net absorption results. The situation changes (i) in the presence of dissipation and (ii) at resonances.

(i) Ionization of atoms and ions (inner ionization) and losses of energetic electrons in the interaction region ("outer

 

ionization") clearly lead to absorption. In terms of Poynting's theorem (1) absorption comes into play by a finite dephasing angle. It has explicitly been shown that ionization may be correctly taken into account by introducing an effective collision frequency $\nu_I$ which phenomenologically acts in the same way as the collision frequency $\nu_{ei}$ [21],

$$\overline{\boldsymbol{j}\cdot\boldsymbol{E}} = \frac{1}{2}\epsilon_0\omega_p^2\frac{\nu_I}{\omega^2+\nu_I^2}\hat{\boldsymbol{E}}\cdot\hat{\boldsymbol{E}}^* \tag{2}$$

in a harmonic field $\boldsymbol{E}=\hat{\boldsymbol{E}}(\boldsymbol{x})\exp(-i\omega t)$; $\omega_p$ is the plasma frequency. Detailed studies on the ionization dynamics of rare gas atoms (inner ionization) in medium-sized clusters ($\sim 10^3$ ions and $\sim$8000 electrons) in the moderate intensity range $I_0 \sim 10^{14}-10^{16}$ W cm$^{-2}$ were undertaken by means of a hierarchical tree code [16]. By combining a linear oscillator with ionization damping, it was possible to reproduce the MD simulations and to interpret them in physical terms. As long as field ionization goes on the oscillator is highly damped and takes on energy which is spent for further ionization and heating. As ionization reduces (diminishing $\nu_I$) absorption drops.

(ii) In spherical clusters Mie resonances occur, the first of which lies at $\omega_0=\omega_p/\sqrt{3}$ (the Clausius-Mosotti or Lorentz-Lorenz polarization of classical electrodynamics). When a linear oscillator passes from an eigenfrequency $\omega_0(t)\gg\omega$ through resonance $\omega_0(t)=\omega$ down to $\omega_0(t)\ll\omega$ the phase of $\boldsymbol{j}=-\partial\boldsymbol{P}/\partial t$ varies from $-\pi/2$ through 0 to $+\pi/2$. An adiabatically driven harmonic oscillator absorbs energy irreversibly only at resonance. At $\omega=\omega_0=$const the amplitude grows linearly in time. For this reason the (linear) Mie resonance at $\omega=\omega_p/\sqrt{3}$ (or somewhat reduced value) has been made responsible for most of the absorption of intense laser radiation in clusters [22]. Owing to fast ionization in the initial stage and gas dynamic expansion later, resonance lasts only for a short time. If $\omega_0(t)$ passes through resonance at the characteristic "speed" $T^{-1}=\partial\ln\omega_0/\partial t$ the amplitude $\hat{\delta}$ of the oscillator $\ddot{\delta}+\omega_0^2(t)\delta=\omega^2\delta_0\exp(-i\omega t)$ is amplified by the factor

$$\frac{\hat{\delta}}{\delta_0} = (\omega T)^{1/2}\left|\int_{-\infty}^{+\infty} e^{i\eta^2}d\eta\right| = (\pi\omega T/2)^{1/2}, \quad \omega T \gtrsim \pi, \tag{3}$$

with respect to the oscillation amplitude of a free particle $\delta_0$ [23]. The integral $|\int_{-\infty}^{\eta} e^{i\eta^2}d\eta|$ yields the familiar Cornu spiral. The finite lifetime of the first (linear) Mie resonance has explicitly been accounted for later and a significant reduction of absorption has been found [24]. Once an undamped linear oscillator runs out of resonance it is no longer capable of absorbing energy irreversibly [see Fig. 2(c) in [16]]. In large clusters resonance can also occur at the rarefying edge all over the expansion phase [25].

In summary, quantitative analytical understanding of enhanced absorption in clusters is limited essentially to linear models which in turn are based on the linear harmonic oscillator driven at resonance, or when out of resonance, damped by dissipative effects, like ionization or outflow of energetic electrons from the interaction region. Unfortunately, the linear resonance frequency $\omega_0$ is much higher than the laser frequency and the absorption process due to loss of particles is subject to very special conditions (see Sec. III). At high laser intensities the collective oscillations become highly nonlinear and the concept of linear resonance, or more generally, of a constant phase with respect to the driving field during an oscillation period, is no longer meaningful. In the nonlinear regime, with $\nu_{ei}\approx 0$, $\nu_I\approx 0$, the problem of collisionless absorption of free electrons reduces to the question of which physical effects lead to a phase shift between $\boldsymbol{j}$ and $\boldsymbol{E}$ differing from $\pi/2$ in Eq. (1) to make absorption possible.

In this paper we give a detailed proof of what makes up the physical essence of collisionless absorption of laser radiation by the free electrons in clusters. As we shall see the required right phase between $\boldsymbol{j}$ and $\boldsymbol{E}$ is accomplished by the effect of nonlinear resonance. The proof is based on the idealized interaction model of a rigid electron sphere, oscillating against the positively charged sphere of the cluster ions ("rigid oscillator"), and three natural variants of it. In its simplest version the model was already used by various authors [26], but in different contexts.

## II. DRIVEN RIGID SPHERE OSCILLATOR

The restoring force $\boldsymbol{F}$ between two interpenetrating homogeneously charged spheres consisting of ions and electrons and having total charges $q_i$ and $-q_e$, respectively, can be written as

$$\boldsymbol{F}(\boldsymbol{x}) = -\boldsymbol{e}_r\frac{q_i q_e}{4\pi\epsilon_0 R_i^2}f(r,\rho), \tag{4}$$

with the symbols $R_i, R_e$ the radii of the ion and electron spheres, $\boldsymbol{x}_i, \boldsymbol{x}_e$ the position vectors of their centers; $\boldsymbol{x}=\boldsymbol{x}_e-\boldsymbol{x}_i$, $r=|\boldsymbol{x}|/R_e$, $\boldsymbol{e}_r=\boldsymbol{x}/|\boldsymbol{x}|$, $\rho=R_i/R_e$. Individual radii $R_i, R_e$ and charges $q_i, q_e$ are introduced to account for expansion of the electron cloud and losses of hot electrons ("outer ionization") during interaction ($R_e\geqslant R_i, q_e\leqslant q_i$). The dimensionless function $f$ is given by

$$f(r,\rho) = \rho^2\times\begin{cases} r & \text{for } r\leqslant 1-\rho,\\ 3(a_1 r^{-2}-a_2+a_3 r-a_4 r^2+a_5 r^4) & \text{for } 1-\rho<r\leqslant 1+\rho,\\ 1/r^2 & \text{otherwise;}\end{cases}$$

$$a_1 = \frac{1}{2}\left[\frac{1}{3}+\frac{1}{48}\left(\frac{1}{\rho^3}+\rho^3\right)-\frac{3}{16}\left(\frac{1}{\rho}+\rho\right)\right], \quad a_2 = \frac{3}{32}\left(\frac{1}{\rho^3}-\frac{2}{\rho}+\rho\right),$$

$$a_3 = \frac{1}{6}\left(\frac{1}{\rho^3}+1\right), \quad a_4 = \frac{3}{32\rho}\left(\frac{1}{\rho^2}+1\right), \quad a_5 = \frac{1}{96\rho^3}. \tag{5}$$

The associated potential $\Phi$, $\nabla\Phi = -\boldsymbol{F}$, $\Phi(0)=0$, is

$$\Phi(\boldsymbol{r}) = \frac{q_i q_e}{4\pi\epsilon_0 R_i}\varphi(r,\rho),$$

$$\varphi(r,\rho) = \rho \times \begin{cases} r^2/2 & \text{for } r \leqslant 1-\rho, \\ 3\left(b - \dfrac{a_1}{r} - a_2 r + \dfrac{a_3}{2}r^2 - \dfrac{a_4}{3}r^3 + \dfrac{a_5}{5}r^5\right) & \text{for } 1-\rho < r \leqslant 1+\rho, \\ \dfrac{3}{10}(5-\rho^2) - 1/r & \text{otherwise.} \end{cases} \tag{6}$$

Here $b=(1-\rho)^2(1+2\rho-2\rho^2-\rho^3)/20\rho^3$. Figure 1 shows $f(r,\rho)$ and $\varphi(r,\rho)$ as functions of $r$ for different values of $\rho$. The dimensionless functions $f(r,\rho)$ and $\phi(r,\rho)$ are invariant under $R_e \to \alpha R_e$ and $R_i \to \alpha R_i$, i.e., when the radii change by the same ratio $\alpha \geqslant 0$. Hence $\boldsymbol{F}(\boldsymbol{x})$ and $\Phi(\boldsymbol{x})$ change as $\boldsymbol{F}(\boldsymbol{x}) \to \boldsymbol{F}(\boldsymbol{x})/\alpha^2$ and $\Phi(\boldsymbol{x}) \to \Phi(\boldsymbol{x})/\alpha$.

The two spheres are bound together by the energy

$$\mathcal{E}_I = \frac{3}{10}\rho(5-\rho^2)\frac{q_i q_e}{4\pi\epsilon_0 R_i}. \tag{7}$$

Since the laser wavelength is at least 1 to 2 orders of magnitude larger than the cluster diameter and the concentration of clusters is low the vacuum values of the laser field $\boldsymbol{E}$ and $\boldsymbol{B}=\boldsymbol{k}\times\boldsymbol{E}$, where $\boldsymbol{k}$ is the wave vector, act on the elementary charges $-e$ and $+Ze$. Then the motion of the electron and ion spheres is governed by $(Z=1)$

$$N_e m_e \frac{d}{dt}\gamma_e \boldsymbol{v}_e = \boldsymbol{F}(\boldsymbol{x}) - N_e e(\boldsymbol{E} + \boldsymbol{v}_e \times \boldsymbol{B}),$$

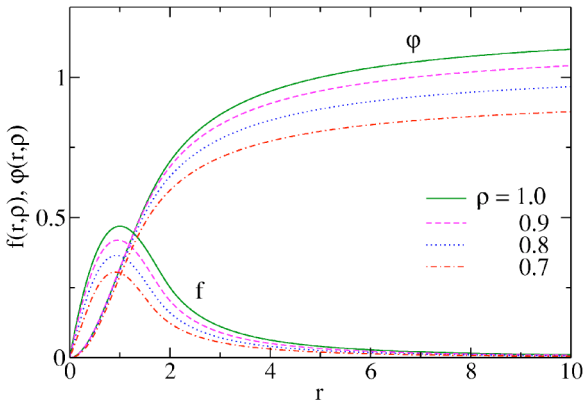


FIG. 1. (Color online) Force and potential terms $f(r,\rho)$ and $\varphi(r,\rho)$ as functions of normalized distance $r$ and ratio of the electron and ion sphere radii $\rho=R_i/R_e$.

$$N_i m_i \frac{d}{dt}\gamma_i \boldsymbol{v}_i = -\boldsymbol{F}(\boldsymbol{x}) + N_i e(\boldsymbol{E} + \boldsymbol{v}_i \times \boldsymbol{B}) \tag{8}$$

where $\gamma_e=(1-v_e^2/c^2)^{-1/2}$ and $\gamma_i=(1-v_i^2/c^2)^{-1/2}$.

The total momentum is not conserved during interaction for two reasons. On the fast time scale of the laser frequency a net force acts on the center of mass owing to retardation. On the slow time scale a ponderomotive force causes a drift of the ions and electrons in the same direction. Hence, contrary to the nonrelativistic case the system of equations (8) cannot be reduced to a single equation for the fast motion in a rigorous sense. However, such a reduction is possible in an approximate way by taking the ions as nonrelativistic and ignoring the ponderomotive force on the fast time scale. Then, with the reduced mass $\mu=N_e m_e N_i m_i/(N_e m_e + N_i m_i)$ and relative velocity $\boldsymbol{v}=\dot{\boldsymbol{x}}_e - \dot{\boldsymbol{x}}_i$ Eqs.(8) reduce to

$$\mu\frac{d}{dt}(\gamma\boldsymbol{v}) = \boldsymbol{F}(\boldsymbol{x}) - N_e e(\boldsymbol{E} + \boldsymbol{v}\times\boldsymbol{B}), \quad \gamma = (1-\boldsymbol{v}^2/c^2)^{-1/2}. \tag{9}$$

The motion is restricted to the plane perpendicular to $\boldsymbol{B}$. The total energy absorbed by the cluster is given by

$$\mathcal{E}_A = \mu c^2(\gamma - 1) + \frac{q_e q_i}{4\pi\epsilon_0 R_i}\varphi(r,\rho). \tag{10}$$

The laser pulse is assumed to propagate in the $x$ direction and is linearly polarized in the $y$ direction, $\boldsymbol{E}=\boldsymbol{e}_y E_0 g(t,x)$, with the structure function $g(t,x)$,

$$g(t,x) = \begin{cases} \sin[(\omega t - kx)/n]\sin(\omega t - kx) & \text{for } 0 \leqslant \omega t - kx \leqslant n\pi, \\ 0 & \text{otherwise.} \end{cases} \tag{11}$$

The pulse contains $n/2$ oscillations. Equation (10) holds for $R_e, R_i, q_e, q_i = \text{const}$ in time. If at least one of them changes during irradiation the absorbed energy must be calculated from the work done by the laser field on the oscillating system,

$$\mathcal{E}_A = -\int_0^{nT_L/2} dt\left(q_e - (q_i - q_e)\frac{\mu}{N_i m_i}\right)\boldsymbol{E}\cdot\boldsymbol{v}. \qquad (12)$$

In an extended cluster medium an absorption coefficient $\alpha_C$ is defined in the same way as $\alpha$ for ordinary matter, i.e., $dI/dx=-\alpha_C I$ (Beer's law). Hence

$$\alpha_C = n_C \mathcal{E}_A/\mathcal{E}_L, \qquad (13)$$

where $n_C$ is the cluster density and $\mathcal{E}_L$ the laser pulse energy incident on the unit area,

$$\mathcal{E}_L = \int_0^{nT_L/2} I\,dt = \frac{1}{2}c\epsilon_0\int_0^{nT_L/2} dt\,E^2(t)$$

$$= T_L I_0 \int_0^{n/2} d\tau \sin^2(2\pi\tau/n) = nT_L I_0/4; \qquad (14)$$

where $I_0=c\epsilon_0 E_0^2/2$ is the peak intensity, $nT_L/2$ the pulse length, and $\tau=t/T_L$. In a weak laser field $r\ll 1$ and with $R_e=R_i=R$, $q_i=4\pi n_e e R^3/3$, the motion of the electron sphere reduces to that of a driven harmonic oscillator with eigenfrequency $\omega_0=\omega_p/\sqrt{3}$, $\omega_p^2=e^2 n_e/\epsilon_0\mu_e$,

$$\frac{d^2y}{dt^2} + \omega_0^2 y = -\frac{e}{\mu_e}E_0 g(t,x), \quad \mu_e = \mu/N_e. \qquad (15)$$

The energy absorbed by the oscillator, $\mathcal{E}_A$, is the sum of potential and kinetic energy residing in the system after the pulse is over. It is generally only a small fraction of the maximum energy of the oscillator during the pulse.

## III. THE ABSORBED ENERGY

The aim is to study the absorption behavior of the oscillator when driven nonlinearly in a relevant parameter domain and, possibly, to determine the maximum of energy conversion.

### A. The free rigid oscillator

First the eigenperiod is evaluated as a function of amplitude $r=x/R_e$, $R_e=$const. With the help of the potential $\Phi(r)$ from Eq. (6) it is determined by

$$T = 4R_e\int_0^{r_{\max}} \frac{dr}{[2(\mathcal{E}_{\rm os}-\Phi)/\mu]^{1/2}}. \qquad (16)$$

The amplitude $R_e r_{\max}$ results from $\Phi(r_{\max})=\mathcal{E}_{\rm os}$. If the total energy approaches the binding energy $\mathcal{E}_I$ the period $T$ tends to infinity. In Fig. 2 $T$ is shown in units of $T_0=2\pi/\omega_0$ for $q_i=q_e=q$ and $\rho=1.0, 0.9, 0.8, 0.7$. The increase of the oscillation period with decreasing $\rho$ is to be expected from Fig. 1. For $\rho\geqslant 0.5$ and amplitudes $\hat{y}=R_e r_{\max}$ exceeding $R_i+2R_e$ the period $T$ increases as $T\sim\hat{y}^{3/2}$. This is according to Kepler's law, which is independent of angular momentum and therefore holds also for ellipses degenerating into a straight line.

### B. The rigid oscillator driven by a harmonic electric field

For easier physical interpretation and to learn about the role of the Lorentz force, in a first stage all calculations are performed by setting the magnetic field $\boldsymbol{B}=\boldsymbol{0}$. The equation governing the motion is

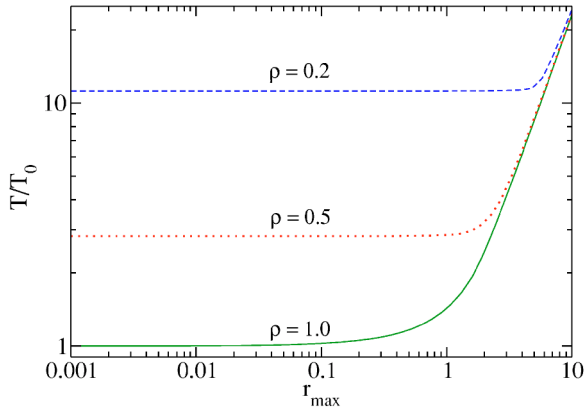


FIG. 2. (Color online) Eigenperiod $T$ of the rigid oscillator as a function of the oscillation amplitude $r_{\max}$ for different values of $\rho$. For $r_{\max}\ll 1$ (harmonic oscillator), $T=T_0/\rho^{3/2}=2\pi\sqrt{3}/(\omega_p\rho^{3/2})$, where $\omega_p$ is the plasma frequency. For $r_{\max}>2-3$, $T\sim r_{\max}^{2/3}$ holds (Kepler's third law).

$$\frac{d}{dt}(\gamma\boldsymbol{v}) + \frac{q_i e}{4\pi\epsilon_0 R_i^2}f(r,\rho) = -\frac{e}{\mu_e}E_0 g(t,x=0). \qquad (17)$$

The dynamics develops in the $y$ direction only; the $x$ coordinate remains fixed. In what follows $x=0$ is set. The energy absorption of the rigid oscillator, Eq. (12), is now studied, if not stated differently, for the following parameters:

$$n_i = n_e = 10^{23}\ \mathrm{cm}^{-3}, \quad q_i = q_e = q = Ne,$$

$$R_i = R_e = R = 20\ \mathrm{nm}; \quad \omega_0 = \omega_p/\sqrt{3} = 1.03\times 10^{16}\ \mathrm{s}^{-1},$$

$$\text{Ti:sapphire laser } \omega = 2.36\times 10^{15}\ \mathrm{s}^{-1} = 0.227\omega_0, \quad n = 10. \qquad (18)$$

#### 1. Weak driver

At low laser intensities the oscillation amplitude lies in the harmonic domain $\hat{y}\ll R$, with $\hat{y}$ the amplitude, with the motion governed by Eq. (15). When it is driven by a pulse of the shape Eq. (11) from $y(0)=v(0)=0$, $v=\dot{y}$, at position $x=0$ it oscillates according to

$$v = \frac{eE_0}{2\mu_e}\left\{A\sin(\omega_1 t) - B\sin(\omega_2 t) + AB\frac{4\omega^2\omega_0}{n\omega_1\omega_2}\sin(\omega_0 t)\right\},$$

$$y = -\frac{eE_0}{2\mu_e}\left\{\frac{A}{\omega_1}\cos(\omega_1 t) - \frac{B}{\omega_2}\cos(\omega_2 t) + AB\frac{4\omega^2}{n\omega_1\omega_2}\cos(\omega_0 t)\right\}, \qquad (19)$$

where $A=\omega_1/(\omega_0^2-\omega_1^2)$, $B=\omega_2/(\omega_0^2-\omega_2^2)$, $\omega_1=(1-1/n)\omega$, $\omega_2=(1+1/n)\omega$, and $n>0$.

The energy absorbed from the pulse by a single electron at $t\geqslant nT_L/2$ follows from Eq. (12),

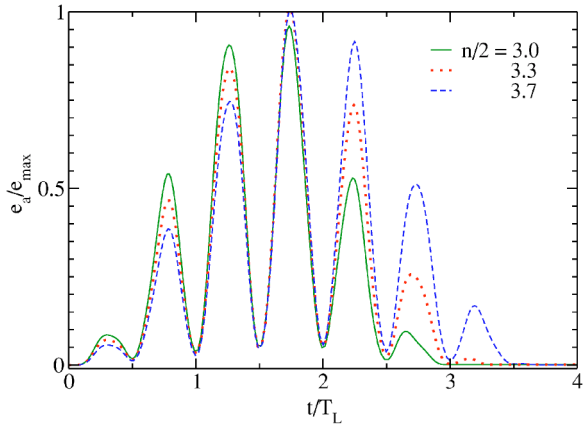


FIG. 3. (Color online) Energy $e_a(t)$ of a harmonic oscillator (eigenfrequency $\omega_0$) driven by a laser pulse $E(t)=E_0\sin(\omega t/n)\sin(\omega t)$, $\omega=2\pi/T_L=0.227\omega_0$ [see Eq. (11)]. Normalization factor $e_{\max}$ from Eq. (20). The laser pulse contains $n/2=3$, 3.3, and 3.7 cycles. In all cases the net absorbed energy $e_a(\infty)$ oscillates between $4.2\times10^{-4}e_{\max}$ and $1.5\times10^{-3}e_{\max}$.

$$e_a=\frac{\mathcal{E}_A}{N}=-e\int_0^{nT_L/2}dt\,E(t)v(t).$$

For an integer value of $n$ the integral of $E$ times the first two terms (driven oscillation) of $v$ in Eq. (19) yields a zero contribution. The result of the free oscillating (third) term of $v$ times $E$ is conveniently expressed in units of the stationary maximum oscillation energy $e_{\max}$ reached after $n/4$ cycles for large $n$,

$$e_{\max}=\frac{\omega_0^2}{2}\frac{e^2E_0^2}{\mu_e(\omega_0^2-\omega^2)^2}. \tag{20}$$

After approximating $(\omega_0^2-\omega_1^2)(\omega_0^2-\omega_2^2)$ by $(\omega_0^2-\omega^2)^2$ the simple expression for $e_a=e_a(t\to\infty)$,

$$e_a\approx\frac{8}{n^2}\frac{\omega^4}{(\omega_0^2-\omega^2)^2}[1-\cos(n\omega_0T_L/2)]e_{\max}, \tag{21}$$

is obtained. Already for $n$ as low as 3 and $\omega=0.227\omega_0$ the net absorption after the pulse is over, according to Eq. (21) is less than $e_a=4\times10^{-3}e_{\max}$. In Fig. 3 the absorbed energy $\mathcal{E}(t)$ is plotted as a function of time for $n/2=3,3.3,3.7$ cycles, i.e., for integer and real $n$, and $\omega=0.227\omega_0$. The result is $e_a/e_{\max}=8.1\times10^{-4}$, $1.5\times10^{-3}$, and $4.2\times10^{-4}$. It shows that the harmonic oscillator, when driven adiabatically, out of resonance does not absorb energy, in agreement with what is well known from quantum mechanics. Owing to the quadratic dependence of $e_a=e_a(\infty)$ on $n$, adiabaticity is reached already with very short pulses. The result Eq. (21) applies in particular to free particles with $\omega_0=0$. The only effect a laser pulse has on a free electron consists in a displacement in the propagation direction by the ponderomotive effect without any change in momentum after the pulse is over. Since this effect exists also for particles with internal degrees of freedom [27], at low intensities a cluster undergoes a small displacement proportional to $(\omega_0^2-\omega^2)^{-1}$.

One may ask now what the effect of an anharmonicity on the harmonic oscillator is. If the anharmonic term is a power of the excursion or a finite sum of power terms, harmonics of the driving frequency are generated, and perhaps secular terms (zero frequency), but no phase shifts, and hence almost no net absorption results in such a case either.

At resonance the situation is peculiar owing to the time-dependent amplitude $-(eE_0/\mu_e)\sin(\omega t/n)$ of the driver which leads to the detuned frequencies $\omega_1$ and $\omega_2$ in Eq. (19). The inhomogeneous part of the solution of Eq. (15) for the driver (11) can be written as ($\kappa=-eE_0/\mu_e$)

$$\begin{aligned}y(t)=&\frac{\kappa}{4\omega_0}\sin\omega_0t\int_0^t dt'\{\cos(\omega_0-\omega_1)t'-\cos(\omega_0-\omega_2)t'\\&+\cos(\omega_0+\omega_1)t'-\cos(\omega_0+\omega_2)t'\}\\&+\frac{\kappa}{4\omega_0}\cos\omega_0t\int_0^t dt'\{\sin(\omega_0-\omega_2)t'-\sin(\omega_0-\omega_1)t'\\&+\sin(\omega_0+\omega_2)t'-\sin(\omega_0+\omega_1)t'\}.\end{aligned} \tag{22}$$

The stationary resonant driver $\kappa\sin\omega_0t$ at $x=0$ is obtained from Eq. (11) for $n$ taken very large in a time interval around $t_0=n\pi/2\omega_0$. It exhibits the well-known particular integral $y(t)=(\kappa/2\omega_0)t\sin\omega_0t$ and the absorbed energy per particle and cycle $e_a(T_L)=-2\pi\kappa e/4\omega_0^2$. For small and moderate values of $n$ exact resonance occurs at either $\omega_1=\omega_0$ or $\omega_2=\omega_0$. In the first case one deduces from Eq. (22)

$$\begin{aligned}y(t)=\frac{\kappa}{4\omega_0}\Bigg\{&\left(t-\frac{n-1}{2\omega_0}\sin\frac{2\omega_0t}{n-1}\right)\sin\omega_0t\\&-\frac{n-1}{2\omega_0}\left(1-\cos\frac{2\omega_0t}{n-1}\right)\cos\omega_0t\Bigg\}.\end{aligned} \tag{23}$$

As a consequence, the absorbed energy at the end of the pulse for integer $n$,

$$e_a(nT_L/2)=\frac{\mu_e}{2}\omega_0^2y^2(nT_L/2) \tag{24}$$

$$=\frac{(n\pi eE)^2}{8\mu_e\omega_0^2}\left[1+\frac{1}{4\pi^2}\left(1-\frac{1}{n}\right)^2\right], \tag{25}$$

is four times less than for the stationary driver above. For $\omega=\omega_0$ the result is $\omega_0-\omega_1=\omega_0/n$, $\omega_0-\omega_2=-\omega_0/n$, and $\omega_0+\omega_1\approx\omega_0+\omega_2\approx2\omega_0\gg\omega_0/n$. Hence apart from two small, fast oscillating contributions, $y(t)$ and $e_a(nT_L/2)$ are now

$$y(t)=-\frac{\kappa}{2\omega_0^2}\left(1-\cos\frac{\omega_0t}{n}\right)\cos\omega_0t,$$

$$e_a(nT_L/2)=\frac{e^2E_0^2}{4\mu_e\omega_0^2}(1-\cos\omega_0T_L/2)=\frac{e^2E_0^2}{2\mu_e\omega_0^2}. \tag{26}$$

Thus, at $\omega=\omega_0$ the absorbed energy is much less than at partial resonance $\omega_1=\omega_0$ or $\omega_2=\omega_0$. The presence of modulations in Eq. (22) indicates that a fraction of the energy absorbed by the linear oscillator close to resonance may be reversibly converted back to the driver.

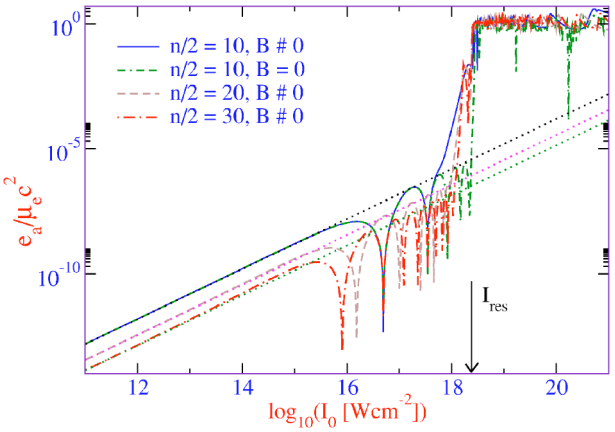


FIG. 4. (Color online) Rigid oscillator ($R_e=R_i=R=20$ nm) driven by the Lorentz force in Eq. (29). Absorbed energy per electron $e_a=e_a(t\to\infty)$ normalized to its rest energy $\mu_e c^2$ as a function of peak laser intensity $I_0$ in W cm$^{-2}$ for pulses containing $n/2=10$, 20, and 30 cycles. Dashed, magnetic field $B=0$; solid, $B$ included; dotted straight lines, harmonic oscillator off resonance ($\omega=0.227\omega_0$). When the oscillator crosses the nonlinear resonance $I_{\mathrm{res}}$ (arrow) $e_a$ increases by a factor $\geqslant 300-10^8$ deterministic chaos).

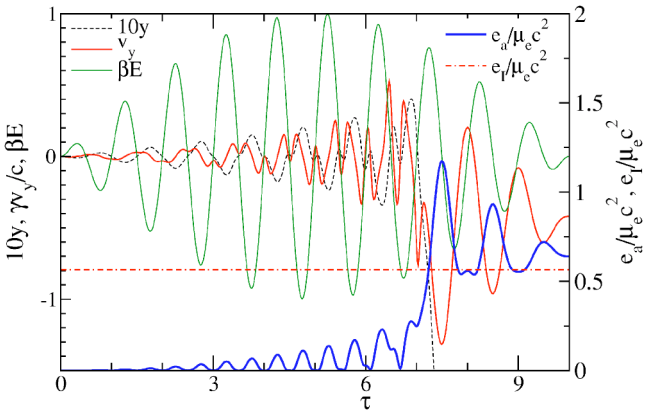


FIG. 5. (Color online) Rigid oscillator ($R=20$ nm), $B=0$. Excursion $y(\tau)$ in units of $\lambda_L$ (magnified by 10), with electric field $E(\tau)$, $\beta$ an arbitrary factor, and absorbed energy $e_a(\tau)$ in units of rest energy $\mu_e c^2$ (bold curve). The horizontal line $e_I=$const marks the average binding energy of an electron (outer ionization potential). Resonance is reached at $I_0=2.75\times10^{18}$ W cm$^{-2}$ and $\tau\approx 6$. All net energy $e_a(\infty)$ is gained during one cycle around resonance. The change of phase by $\pi$ between $v_y$ and $E$ is clearly seen by comparing $v_y$ and $y$ with $E$ before and after resonance.

### *2. Nonlinear resonance and the origin of phase shift*

As the amplitude increases with the driver strength $E_0$ the effective oscillation frequency (16) $\omega_{\mathrm{eff}}=2\pi/T$ decreases in agreement with what one predicts from Fig. 2. Thus it is possible to study the behavior of absorption and dephasing of $\boldsymbol{j}$ relative to $\boldsymbol{E}$ of the rigid oscillator at resonance $\omega_{\mathrm{eff}}=\omega$ by choosing $E_0$ appropriately and by determining $\int_0^t dt' vE$ as a function of time.

In Fig. 4 the net energy $e_a$ of the rigid oscillator irreversibly extracted form the laser is plotted as a function of the peak laser intensity $I_0=\epsilon_0 c^2 E_0^2/2$ (dashed curve). In the linear regime ($I_0<10^{14}$ W cm$^{-2}$) the absorbed fraction $e_a/I_0 \sim e_a/e_{\max}$ is very low as it should be according to Eq. (21) out of resonance ($\omega=0.227\omega_0$). A strong, steplike increase of $e_a$ by 2 orders of magnitude occurs at $I_0=2.75\times10^{18}$ W cm$^{-2}$ where $\omega_{\mathrm{eff}}=\omega$ is reached at the maximum of the pulse. In Fig. 5 the time history of $y$, $v$, $E$, and $e_a(t)=-e\int_0^t dt' vE$ is shown for intensities $I_0$ around the first resonance. The graphs of $e_a(t)$, together with that of $e_a=e_a(\infty)$ from Fig. 4, show, very much in analogy to the absorption behavior of the linear oscillator, (1) almost no "positive," i.e., absorptive, dephasing between $v$ and $E$ before resonance, i.e., $e_a(t<t_{res})\approx 0$; (2) strong positive dephasing at nonlinear resonance $\omega_{\mathrm{eff}}\approx\omega$; and (3) that a major part of the energy pumped into the oscillator at resonance is reversible on the average; only a smaller fraction of it appears as net absorption $e_a(\infty)$ when the pulse is over.

The spikes in Fig. 4 and the modulational evolution of $e_a(t)$ in Fig. 5 are not surprising because they are present to a minor degree already in the formulas of Sec. III B 1.

When the electron sphere remains bound after resonance ($\mathcal{E}_A<\mathcal{E}_I$), it enters a second resonance on the decaying side of the pulse. Its contribution to $e_a$ depends crucially on the phase of $v$ at this second entrance. The spiky graph of Fig. 4 at the right-hand side of the resonance exhibits constant energy, i.e., no energy gain, against increasing $I_0$. This is to be expected from the fact that the resonance of Fig. 5 shifts to the left with increasing $I_0$. The plateau does not depend on the pulse length. This has been tested with a driver given by (11) but the number of cycles $n/2=10$, 20, and 30. The only changes are limited to the spacing of the spiking fine structure at $I_0>I_{\mathrm{res}}$. This behavior is an additional proof that the energy gain takes place only during one cycle approximately at resonance.

There is still an open question: Does positive dephasing with the rigid oscillator occur only at resonance or also beyond resonance, $t>t_{\mathrm{res}}$? That there is no such dephasing for $t<t_{\mathrm{res}}$ and for the whole laser pulse interval $nT_L/2$ for $I_0<I_{\mathrm{res}}$ has already been seen from Figs. 4 and 5. By comparing with the linear oscillator it is clear that a positive (i.e., absorptive) dephasing for $t>t_{\mathrm{res}}$ can originate, if at all, only from the nonlinearity of the rigid oscillator. The question can be answered only by analyzing the dephasing between $v$ and $E$ at higher intensities. Numerous computer runs with a whole variety of parameters (intensity, driver frequency, pulse length) give, with respect to phase shift, an identical answer as Fig. 6 for $I_0=6.0\times10^{18}$ W cm$^{-2}$. Except for the narrow interval of resonance of duration $T\lesssim 2\pi/\omega$ around $t=t_{\mathrm{res}}\approx 3.5$ cycles the phase difference between $v$ and $E$ is $\pi/2$ everywhere. An additional result is that the irreversibly absorbed energy varies considerably as the parameters are changed only by small amounts, i.e., the driven rigid oscillator evolves into chaos. A careful study of the pertinent Lyapunov exponents (to be published elsewhere) confirms the hypothesis. In nearly all cases the energy at the end of the pulse is lower than at the end of resonance $t=t_{\mathrm{res}}+\epsilon$,

$$-e\int_0^{t_{\mathrm{res}}+\epsilon} dt\, vE > -e\int_0^{nT_L/2} dt' vE. \tag{27}$$

The inequality is inverted in the rare cases where the oscillator enters the second resonance point with the right phase.

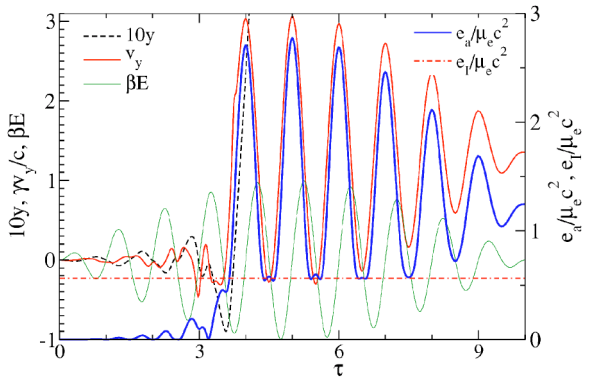


FIG. 6. (Color online) Rigid oscillator, $B=0$, at $I_0=6.0\times10^{18}$ W cm$^{-2}>I_{\rm res}$. Resonance threshold is crossed at $\tau\approx3$ within one cycle with phase shift by $\pi$. There are no contributions to $e_a(\infty)$ beyond $\tau_{\rm res}$. Units and symbols as in Fig. 5.

From the analysis we conclude that (1) irreversible energy absorption by the rigid oscillator occurs at nonlinear resonances; and (2) absorptive dephasing between $\boldsymbol{j}$ and $\boldsymbol{E}$ is limited to the crossings of resonances. Neither nonlinearities nor asymmetric excitation of the cluster [see $y(t)$ and $v(t)$ for $t>t_{\rm res}$ in Figs. 4 and 5] leads to collisionless absorption.

To test the accuracy of the numerical integration procedure time reversal $t\rightarrow-t$ at the end $t=nT_L$ of the laser pulse was carried out. The result was very satisfactory in all cases, even across the resonance.

So far all numerical calculations were done with clusters having the size of $R=20$ nm. From the scaling law of the eigenperiod $T$ on $R$ in Sec. III A it follows that for a cluster of size $\alpha R$ to be at resonance $T_{\rm res}=2\pi\omega_{\rm eff}=0.227\omega_0=$const,

$$\alpha^{3/2}[\varphi(r_{\rm max})]^{-1/2}=\text{const}, \tag{28}$$

or $\varphi(r_{\rm max})=\varphi(I_0)\sim\alpha^3$ must be satisfied. Unfortunately, this implicit equation can be solved only numerically. In Fig. 7 $I_{\rm res}=I_0$ is plotted for smaller clusters as a function of $\alpha$. For clusters of half the standard size, $R=10$ nm, resonance occurs at $I_0=6.96\times10^{17}$ W cm$^{-2}$.

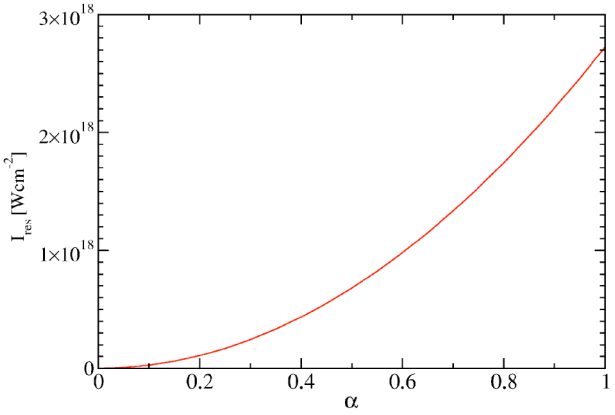


FIG. 7. (Color online) Resonance threshold $I_0$ W cm$^{-2}$ as a function of cluster size $R_e=R_i=\alpha R$, $R=20$ nm, $\omega=0.227\omega_0$, $\boldsymbol{v}\times\boldsymbol{B}$ neglected.

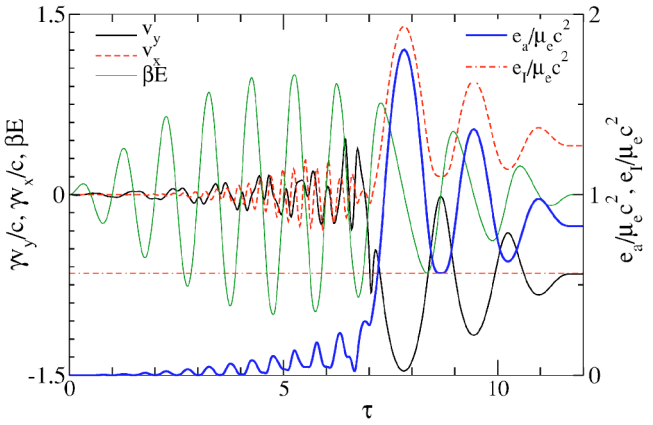


FIG. 8. (Color online) Rigid oscillator, $B$ included. Resonance shifts from $I_0=2.75\times10^{18}$ ($B=0$) to $2.60\times10^{18}$ W cm$^{-2}$. Period lengthening is due to longitudinal Doppler effect. Velocities $v_x$ and $v_y$ are of the same order of magnitude. Units as in Fig. 5.

### *3. The effect of the Lorentz force on the rigid oscillator*

The cycle-averaged oscillation energy of a free electron $\mathcal{E}_{\rm os}=m_ec^2[(1+a^2/2)^{1/2}-1]$, $a=eE_0/m_e\omega c$, in a Ti:sapphire laser beam equals the rest energy of the electron at $a=6$, corresponding to $I_0=6.5\times10^{18}$ W cm$^{-2}$. Therefore one could be tempted to conclude that the hitherto ignored Lorentz force should not play an important role for laser-cluster interaction below $I_0\approx10^{18}$ W cm$^{-2}$. As is shown now this is not true for several reasons.

The equation of motion to be solved is

$$\frac{d}{dt}(\gamma\boldsymbol{v})+\frac{eq_i}{4\pi\epsilon_0\mu_eR_i^2}f(r,\rho)=-\frac{e}{\mu_e}E_0\left(1+\boldsymbol{v}\times\frac{\boldsymbol{e}_z}{c}\right)g(t,x). \tag{29}$$

Since the motion takes place also in the $x$ direction, in addition to the transverse excursion along the $y$ axis, the longitudinal Doppler effect leads to laser period dilation [$v_x(t)>0$] and contraction [$v_x(t)<0$], and to significant distortion in time of the sinusoidal driver field. Figure 8 illustrates the difference from Fig. 5 at the threshold of the resonance intensity which lies now at the slightly lower value $I_{\rm res}=2.6\times10^{18}$ W cm$^{-2}$. The lowering is a consequence of the period lengthening at $t\gtrsim t_{\rm res}$, clearly seen in the figure. As long as the electron sphere is bound, $t<t_{\rm res}$, $v_x$ oscillates at $2\omega$. In the direction $y$ of the electric field the period is $\omega$. The apparent $2\omega$ structure of $v_y$ before resonance is due to a disruption caused by the $v_xB_y$ contribution to $v_y$ because it is of opposite sign. The stretching of the driver field becomes very pronounced well above threshold at $I_{\rm res}=6\times10^{18}$ W cm$^{-2}$ in Fig. 9. Absorptive dephasing is limited again to the resonance transition. Whereas the absorbed energies at the threshold $I_{\rm res}$ in Figs. 5 and 8 are the same, in Fig. 9 it is by 13% higher than in Fig. 6. With a look at the solid line (Lorentz force included) and the dashed line ($B=0$) in Fig. 4 the fraction of absorption increases by 15–20% due to the effect of the magnetic field. In addition the spiky structure for $I_0>I_{\rm res}$ is more pronounced than without $B$. At $I_0<I_{\rm res}$ the Lorentz force leads to partial suppression of structures.

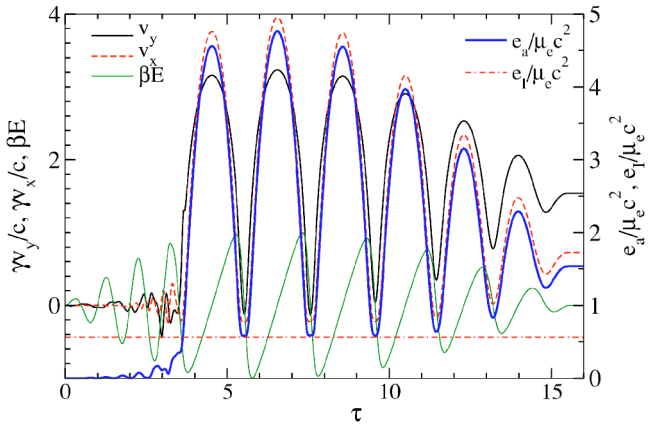


FIG. 9. (Color online) Rigid oscillator, $B$ included. $I_0=6.0\times10^{18}$ W cm$^{-2}$; to be compared with Fig. 6. Period lengthening is very pronounced; phase shift at resonance is clearly seen. Units as in Fig. 5.

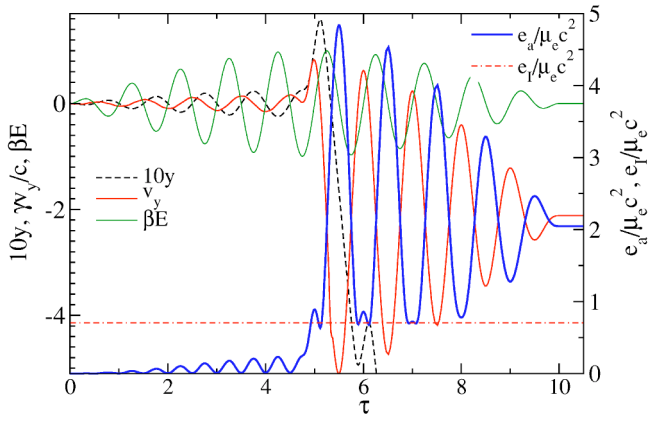


FIG. 10. (Color online) Single electron in static ion field at resonance threshold $I_0=1.8\times10^{19}$ W cm$^{-2}$, $B=0$. The electron starts at $x_0=0$, $y_0/R=0.01$. Owing to the high ion potential, $I_{\rm res}$ is 6.5 times higher than in Fig. 5. Apart from this, its behavior is similar to the rigid oscillator at its resonance threshold. Units as in Fig. 5.

Beyond resonance there is a tendency for $|v_x|$ to become larger than $|v_y|$ (e.g., in Fig. 9); however, at the threshold $I_0=I_{\rm res}$ it is not true (see Fig. 8). Below the outer ionization threshold $I_{\rm res}$ the electron sphere is bound and the amplitudes $\hat{v}_x$ and $\hat{v}_y$ are of the same magnitude. As a consequence of the central force deviating from a $1/|\boldsymbol{x}|^2$ law and the presence of the driver the orbits are no longer closed, and rotate. This causes the kinetic energy to oscillate between the $x$ and $y$ directions. The eigenperiod of the free oscillator $T$ of Fig. 8 undergoes almost no change because it is solely a function of the major half axis of the Kepler-like orbit.

The majority of PIC or MD simulations were using pure electrostatic codes and linearly polarized laser fields [18–20,22,26,28,29]. The interplay of the driver with the polarization and space charge fields in combination with the cluster geometry (i.e., driver and electrostatic fields exhibit different symmetry) lead to some degree of randomization of the electrons leaving the cluster; however, there is also a clear signature, common to all of these simulations, of a favored polarized motion in the direction of the electric laser field. From the model calculations described in this subsection we conclude that the Lorentz force greatly enhances directional randomization due to mixing of the electron dynamics along different directions. The Lorentz force may be important already at intensities $I_0<10^{17}$ W cm$^{-2}$ owing to the resonant increase of $v_y$ in small and/or expanding cluster electron clouds (see below).

### C. Alternative oscillators

So far the rigid oscillator model has shown that collisionless energy absorption takes place when the electron sphere is driven through the nonlinear resonance. There are tidal forces acting on the various regions of this sphere because portions adjacent to the quasistatic sphere of ions experience a stronger attraction than portions in the opposite location; after half an oscillation period of the electron sphere the situation is inverted. As a consequence of such modulational forces varying from point to point local space charges are induced which lead to a rapid disassembly of the outer shell of the "rigid" electron sphere, as manifested in PIC simulations. The tidal forces are stronger in larger clusters and reach, each portion individually, a maximum for an excursion $r$ lying in the nonlinear domain of oscillation. At vanishing excursion $r\ll1$ the tidal forces are limited to the borders lying outside the ion sphere whereas all parts lying inside experience the constant Clausius-Mosotti space charge field $E=P/3\epsilon_0$. In small clusters tidal forces and space charges play a subdominant role, also because their equilibrium electron charge is low [30].

The main purpose of the paper is to prove the hypothesis raised by us that the electrons, after having been set free by inner ionization, gain their additional energy from crossing resonances. In this way one is led directly to the two alternative models of (1) one single electron in the field of the ion sphere driven by the laser field and (2) a single electron moving under the combined field of the laser and driven rigid oscillator of Sec. II. In this second case the single electron moves in the static field of the ion sphere under the action of two drivers, the nonautonomous external driver, and the autonomous field of the oscillating electron sphere. It is given the name "modal oscillator."

#### *1. Single electron in the static ion field*

The test electron starts at $t=0$ from a given position $\boldsymbol{x}_0$ with velocity $\boldsymbol{v}=\boldsymbol{0}$. The laser field is taken from Eq. (11); the additional force is represented by the attraction of the ion sphere of charge $q_i=q$,

$$\boldsymbol{F}(r)=-\boldsymbol{e}_r\frac{eq}{4\pi\epsilon_0R_i^2}\begin{cases}r, & r\leqslant1,\\ 1/r^2, & r>1.\end{cases}\tag{30}$$

In order to have a direct comparison with the results of the foregoing section use is made of the parameters from Eq. (18). An electron starting from $x_0/R=0$ and $y_0/R=0.01$ encounters the nonlinear resonance at $I_{\rm res}=I_0=1.8\times10^{19}$ W cm$^{-2}$, i.e., at a 6.5 times higher intensity than for the rigid oscillator (Fig. 10). Apart from this in all essential aspects

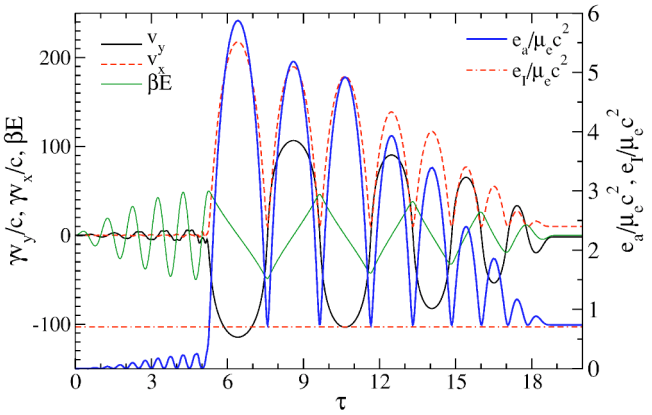


FIG. 11. (Color online) Single electron in static ion field at resonance threshold $I_0=1.68\times10^{19}$ W cm$^{-2}$, $B\neq0$; to be compared with Fig. 8. Units as in Fig. 5.

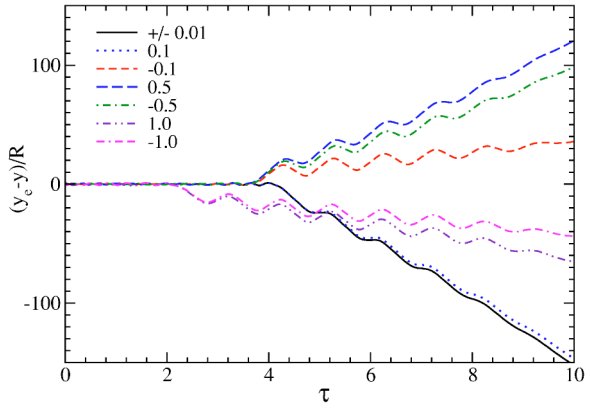


FIG. 12. (Color online) Single-particle motion in the laser-driven modal oscillator: driving field $E$ is the sum of the laser field $E_L$ and the field of the electron sphere, i.e., $E(t)=E_L(t)+E_e(t)$. $y_e(t)$ is the coordinate of the single oscillator, $y(t)$ the center of the oscillating electron cloud; initial positions are $x_0/R=0$, $y_0/R=\pm0.01$, $\pm0.1,\pm0.5,\pm1.0$. $I_0=2.6\times10^{18}$ W cm$^{-2}$, $B=0$. Note that the drift, i.e., average velocity, does not change its slope.

the figure very much resembles Fig. 5. In particular, all energy is gained from the field during one cycle at $t_{\rm res}(\tau=5)$ and the phase shift of $v_y$ relative to $E$ by $\pi$ is clearly seen. In addition, asymmetric excitation beyond $t_{\rm res}$ does not lead to any additional energy gain. As the initial position $\boldsymbol{x}_0$ shifts outward $I_{\rm res}=I_0$ is gradually reduced and at the border of the ion charge $(x/R=0, y/R=1.0)$ it becomes as low as $I_0=1.2\times10^{18}$ W cm$^{-2}$. With the magnetic field included [driver according to Eq. (29)] the resonance for the initial conditions of the Fig. 10 lies now at $I_0=1.68\times10^{19}$ W cm$^{-2}$ (Fig. 11). Both velocities $v_x$ and $v_y$ are of comparable magnitude, which leads to a very pronounced Doppler effect. For the irreversible energy gain and the phase shift the same holds as for $B=0$. The absorbed energy $e_a$ between Figs. 10 and 11 differs by a factor of 3. A slight change of the driver may invert the situation. Averaging $e_a$ over numerous runs with $B=0$ and $B\neq0$ did not show any pronounced trends in the energy ratios. Again, shifting the initial position toward the border of the cluster at $B\neq0$ brings the electromagnetic driver gradually down to the minimum $I_{\rm res}=I_0=1.1\times10^{18}$ W cm$^{-2}$. With respect to energy absorption and phase shifts nothing changes due to the presence of $B$. The conclusions from Sec. III B 2 can be extended to the single-electron oscillator also.

### *2. Modal oscillator*

The modal oscillator represents a suitable tool to study the motion of single electrons starting at velocity zero from different positions. At the same time this modal oscillator is close to reality in so far as it follows the motion of the particle in the two basic fields in a plasma, i.e., the regular external driver and the intense collective field of the entire ensemble of the charges. In Fig. 12 the trajectories relative to the excursion of the electron cloud $y_e-y$ are plotted for seven different initial positions, with the electrostatic driver $(B=0)$ at $I_0=2.6\times10^{18}$ W cm$^{-2}<I_{\rm res}$ and $q_e=q_i=q$. After four cycles symmetric electron diffusion sets in for all initial positions and at the end of the pulse of ten cycles the electrons have moved away from the cluster by nearly 200 cluster radii $R$ (average value $\approx100R$). When the Lorentz force is included it is convenient to plot the distance $[(x_e-x)^2+(y_e-y)^2]^{1/2}$ from the center of the oscillating electron cloud. For $I_0=2.59\times10^{18}$ W cm$^{-2}$ these quantities are shown in Fig. 13 for the same initial conditions as in the Fig. 12, but $q_e=q_i/2$ now. The result is about the same as before. Rapid particle diffusion is to be expected from the PIC simulations. A more detailed analysis shows also that, due to the $B$ field, diffusion in the $x$ direction occurs with the same speed as in the $y$ direction.

There is a significant aspect which emerges form both pictures, i.e., each of the individual particles suddenly acquires, during one cycle, almost its final drift energy, in both the $x$ and $y$ directions (separately proved), indicating in this way that the energy gain is due to transiting locally a reso-

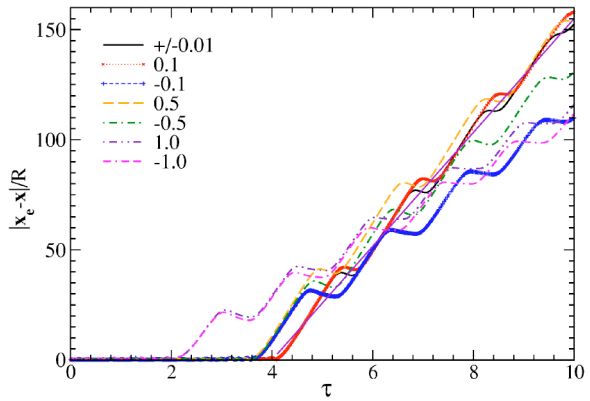


FIG. 13. (Color online) Single-particle motion in the laser-driven modal oscillator with Lorentz force included. Separation $|\boldsymbol{x}_e-\boldsymbol{x}|/R=[(x_e-x)^2+(y_e-y)^2]^{1/2}/R$. $\boldsymbol{x}(t)$ is the center of the oscillating electron sphere; initial positions as in Fig. 12; $I_0=2.59\times10^{18}$ W cm$^{-2}$. Note that the final drift velocity is acquired in a single acceleration event, i.e., at its local resonance (see straight solid line).

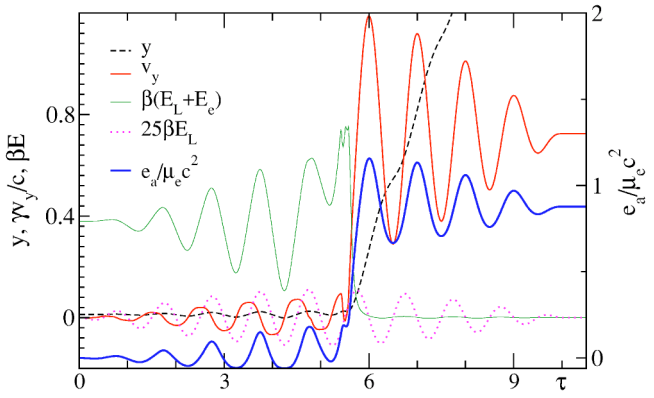


FIG. 14. (Color online) Modal oscillator, i.e., single electron driven by the laser field $E_L$ and the space charge field $E_e$ of the oscillating electron sphere. $I_0=5.0\times10^{17}$ W cm$^{-2}$, $B=0$, initial position $x_0/R=0.0$, $y_0/R=0.5$. The final energy $e_a(\infty)$ is entirely gained during one cycle at $\tau\approx6$; the resonant type of coupling is proved by the phase jump by $\pi$ of velocity $v_y$ and position $y$ in the interval $5<\tau<7$. Units as in Fig. 5.

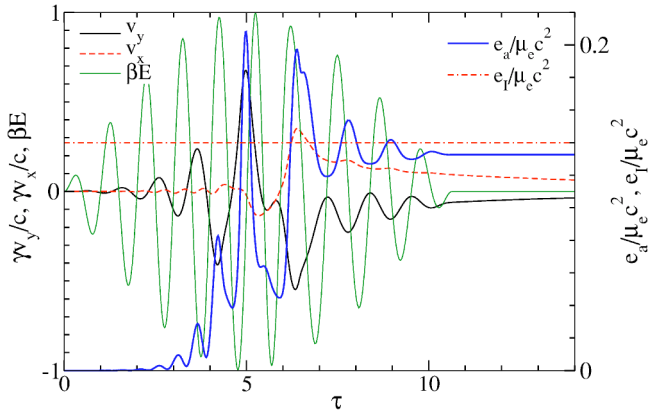


FIG. 15. (Color online) Resonant energy gain of the rigid oscillator with uniformly expanding electron cloud from $R_f=R_i=20$ nm at $\tau=0$ to $R_f=5R_i$ at $\tau=10$. Laser intensity $I_0=5.0\times10^{16}$ W cm$^{-2}$. Resonance occurs in the harmonic regime. Dashed horizontal line indicates the outer ionization energy $e_I$; the electron sphere remains bound $[e_a(\infty)<e_I]$. Units as in Fig. 5.

nance in the combined field of the ion and the displaced electron clouds. The proof of this assertion to be the correct interpretation is given in Fig. 14. The time history of position and velocity $v_y$ of an individual electron starting at $x_0/R=0.0$, $y_0/R=0.5$ is depicted for the laser intensity $I_0=5.0\times10^{17}$ W cm$^{-2}$ and $B=0$; the driver $E=E_L+E_e$. Resonance occurs at $\tau\approx6$ where all energy is gained during one cycle. The change of phase by $\pi$ between $E$, $v$, and $y$ can be pursued in the neighborhood of resonance, $5<\tau<7$. The oscillating space charge field $E_e$ is larger than the laser field before the electron has escaped. The irreversible energy gain (drift) in all other cases occurs in combination with a phase jump by $\pi$ during one oscillation as well.

### *3. Expanding rigid oscillator*

Slight changes of parameters may drastically change the amount of absorbed energy by the rigid oscillator; see in particular Fig. 4. In PIC simulations or experiments such anomalies are not observed owing to the presence of smoothing effects, such as averaging over clusters of different sizes in the experiment, smoothing due to thermal expansion of the electron and, eventually, also of the ion cloud, and smoothing by successive resonances of local bunches of electrons (tidal effects). To complete the present investigation on nonlinear resonance absorption we study characteristic changes due to the expansion of the electron cloud in the rigid oscillator model.

To this end the electron sphere is assumed to increase its radius $R_e$ according to a linear law,

$$R_e = R_i + v_0 t, \tag{31}$$

with a linear radial velocity flow profile, $v_e=\eta r$. The linear profile guarantees the uniform charge distribution within the sphere. The expansion velocity $v_0$ of the border is a free parameter varying typically between the ion and the electron sound speed. From Fig. 1 and from Eq. (16) it is expected that, in addition to smoothing, expansion will considerably facilitate resonance of the rigid oscillator at lower laser intensities. In Fig. 15 the time evolution of the rigid oscillator with the electron sphere expanding now according to Eq. (31) from the initial radius $R_i=20$ nm to the final radius $R_f=100$ nm at $\tau=10$ is shown. $I_0=5.0\times10^{17}$ W cm$^{-2}$ and $B\neq0$. The maximum energy gain is centered at $\tau\approx4.5$ when the electron cloud has expanded by the factor $1/\rho=3$. The oscillation amplitude is much smaller than $R_f$ in this case and hence resonance occurs at the harmonic frequency $\omega_0(\tau=4.5)$ which according to Eq. (5) is reduced by $\rho^{3/2}$. This means $\omega_{\rm res}=\omega_0(\tau=4.5)=\rho^{3/2}\omega_0(\tau=0)=0.21\omega_0(\tau=0)$. This value is in good agreement with the driver frequency ratio of 0.227 used throughout this paper. The energy $e_a(t)$ is to be calculated according to

$$e_a(t) = -e\int_0^t dt\, v_y(E_L - v_x B + E_i), \tag{32}$$

where $E_i(t)$ is the time-dependent average electric field of the rigid ion sphere acting on the single electron of the expanding electron sphere. The expansion is stopped at $\tau=10$. A very similar result is obtained with an overall expansion by the factor $1/\rho=25$ during the laser pulse delivering $I_0=10^{17}$ W cm$^{-2}$. The main differences are an earlier crossing of the linear resonance point, as expected, and a more pronounced increase of velocity $v_y$ for $\tau>10$ owing to slow oscillations in the shallow potential $[e_a(\infty)<e_I]$.

The general scaling of nonlinear resonance absorption in big clusters under simultaneous expansion of the rigidly oscillating electron could is shown in Fig. 16 as a function of the laser strength for three degrees of expansion, $R_f=1.5R_i$, $2R_i$, and $25R_i$, respectively, with the Lorentz force taken into account (bold graphs) and without (thin graphs). For comparison, the situation for $R_f=R_i$ is also shown. It is identical to the corresponding graph in Fig. 4. The dotted diagonal straight line refers to the linear oscillator with $\omega_0=$const (no

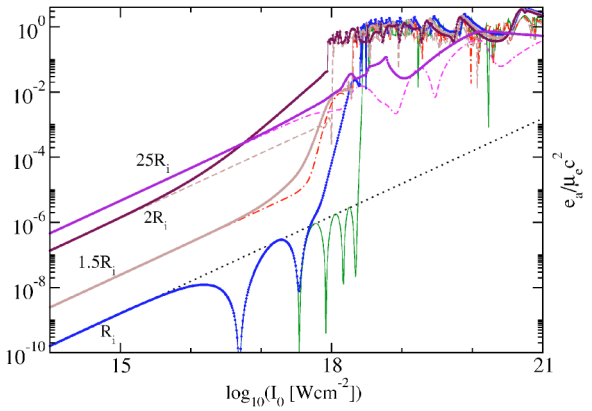


FIG. 16. (Color online) Irreversible energy gain $e_a(\infty)$ as a function of the laser intensity of the rigid oscillator with uniform expanding electron sphere of initial radius $R_i=20$ nm and final radii $R_f=R_i$, $1.5R_i$, $2R_i$, and $25R_i$. Bold solid graphs with Lorentz force included, thin solid and dashed curves without $B$; dotted line refers to the harmonic oscillator out of resonance. Due to expansion resonance structures of Fig. 4 are softened (at $R_f=25R_i$ almost disappeared) and downshifted on the $I_0$ axis; initially $\omega/\omega_0=0.227$.

resonance). As a consequence of expansion $\omega_0(t)$ approaches $\omega$ by dilution [see Eq. (5)], in addition to the power shift of $\omega_0$ according to Eq. (16), and the concomitant gradual smoothing and downshift of the resonance profile. For $R_f=25R_i$ the onset of resonance is no longer detectable in this figure. However, by close inspection and comparing with the aforementioned time history for $R_f=25R_i$ a change in the slope of the curve indicating resonance is detected at $I_0=8.0\times10^{16}$ W cm$^{-2}$.

This concludes the proof of our assertion that collisionless absorption after the electrons have been set free by inner ionization in clusters is due to nonlinear resonance.

## IV. DISCUSSION AND CONCLUSION

The excellent coupling of laser beams with matter in its clustered form is a well-established fact, experimentally as well as by PIC and MD simulations. However, it is an equally incontestable fact that the physical understanding of absorption by the freed electrons in the cluster is rather poor. All analytical models hitherto presented are based on linear resonances. Since linear resonance frequencies are generally much higher than the laser frequency, coupling is imagined to become good only after adequate dilution by expansion of the cluster plasma, e.g., in the case of the fundamental Mie resonance at $\omega_p/\sqrt{3}$, or by the assistance of multiphoton resonance, i.e., the appearance of the third laser harmonic $3\omega$ which may eventually lie close to $\omega_p/\sqrt{3}$ [31]. This latter model is also a linearized concept in its nature and the mechanism is not straightforward enough as to be very efficient. In addition to such considerations the collisionless absorption is not understood so far despite some attempt to explain its underlying physical principle. In connection with clusters the expression "laser dephasing heating" has been coined and has been addressed as the physical mechanism. On closer inspection, however, dephasing is the basis of all kinds of absorption, without exception, since the only access to it, according to Maxwell's equations, regardless whether in classical or in a quantum mechanical version, is through Poynting's theorem, Eq. (1). A valid explanation of where such a dephasing comes from with free electrons has never been given so far.

With the help of the rigid oscillator model in its various versions we were able to show that nonlinear resonance is the physical mechanism leading to the compulsory dephasing needed for absorption in Eq. (1). Free electrons or entire bunches of them oscillate, depending on geometry, in the neighborhood of the plasma frequency under infinitesimal displacements. At increasing separation from each other (large amplitude) the restoring force becomes Coulomb-like with an enormous increase of the oscillation period as quantified by Eq. (16). In other words, at sufficient laser power the cluster eigenperiod, or several eigenperiods of it, are brought down to direct resonance with the laser period $T_L=2\pi/\omega$. In an early stage of collisionless interaction, still overlapping with ionization or not, it may happen in big clusters that only the region at the surface is already driven into resonance and that the inner parts enter this stage later. In any case, as a straightforward process nonlinear resonance is very effective. In our interpretation it is this nonlinear resonance which causes the sudden acceleration of electrons at the border of the cluster and their subsequent ejection, observed in MD simulations of small clusters as well [20].

The concept of resonance brought up in this paper may serve as a basis for forthcoming models which will allow the approximate calculation of the electron distribution function and the effective electron temperature $T_{e,\mathrm{eff}}$ of the heated clustered matter. "Freed" electrons by inner ionization, whether embedded in a macroscopic space charge field or completely free, represent oscillators of linear or nonlinear type. From a quantum mechanical point of view it is rather evident *a priori* that such systems can gain energy irreversibly only at resonance. Thus, it becomes nearly obvious *a posteriori* that "free" electrons in extended smooth fields can gain energy solely by going through a resonance. As we have shown in Sec. III nonlinearities or asymmetries themselves do not lead to absorption.

Particle collisions also lead to dephasing [see Eq. (2)]. Thereby it makes no difference, in principle whether an electron interacts with the field generated by another particle or a field of collective origin. Therefore, sometimes collisionless absorption has been attributed to collisions with fluctuating macroscopic fields. Such fields, however, can act like collisions only if their duration on the particle is shorter than $T_L/3$; any interaction of longer duration falls into the class of adiabatic processes which are reversible [32]. The main fluctuations are concentrated around $\omega_p$ and have spatial extensions larger than a Debye length $\lambda_D$. From kinetic theory it is well known that for all impact parameters $b>\lambda_D=v_{\mathrm{th}}/\omega_p$, where $v_{\mathrm{th}}$ is the average velocity, collisions become inefficient. Thus, the collision time must obey the inequality $\tau_{\mathrm{coll}}<\min(T_L/3,\lambda_D/v_{\mathrm{th}})=\min(2/\omega,1/\omega_p)$. There is no doubt that field fluctuations of collisional character contribute to heating of clusters; their contribution, however, is small. In PIC simulations a kind of threshold behavior of absorption has been observed by various authors [18,19,26,28]. The

rigid oscillator model makes such a threshold well understandable. It is particularly pronounced in [26] where a simplified version of this model was introduced. In addition, at high laser intensities ($I_0 \geqslant 10^{18}$ W cm$^{-2}$) excellent agreement of this model with their PIC simulations was found. Especially in view of Figs. 12 and 13 such a degree of agreement is surprising and represents a not yet well understood fact.

Summarizing we conclude that (i) nonlinear resonance is a leading absorption process in clusters; (ii) without crossing a resonance point nonlinear collisionless interaction is inefficient; (iii) the Lorentz force does not substantially alter the behavior of resonance however, it plays an important role in thermalization of electrons.

## ACKNOWLEDGMENT

One of the authors (M.K.) would like to acknowledge the generous financial support by Prof. D. H. H. Hoffmann during the development of this work.

[1] A. McPherson, B. D. Thompson, A. B. Borisov, K. Bayer, and C. K. Rhodes, Nature (London) **370**, 631 (1994).
[2] T. Ditmire, T. Donnelly, R. W. Falcone, and M. D. Perry, Phys. Rev. Lett. **75**, 3122 (1995).
[3] E. M. Snyder, S. A. Buzza, and A. W. Castleman, Jr., Phys. Rev. Lett. **77**, 3347 (1996).
[4] T. Ditmire, J. W. G. Tisch, E. Springate, M. B. Mason, N. Hay, R. A. Smith, J. Marangos, and M. H. R. Hutchinson, Nature (London) **386**, 54 (1997); T. Ditmire, J. W. G. Tisch, E. Springate, M. B. Mason, N. Hay, J. P. Marangos, and M. H. R. Hutchinson, Phys. Rev. Lett. **78**, 2732 (1997).
[5] G. Grillon *et al.*, Phys. Rev. Lett. **89**, 065005 (2002); J. Zweiback *et al.*, Phys. Plasmas **9**, 3108 (2002).
[6] M. Lezius, S. Dobosz, D. Normand, and M. Schmidt, Phys. Rev. Lett. **80**, 261 (1998); T. Ditmire, E. Springate, J. W. G. Tisch, Y. L. Shao, M. B. Mason, N. Hay, J. P. Marangos, and M. H. R. Hutchinson, Phys. Rev. A **57**, 369 (1998).
[7] S. Dobosz *et al.*, J. Exp. Theor. Phys. **88**, 1122 (1999).
[8] B. D. Thompson, A. McPherson, K. Boyer, and C. K. Rhodes, J. Phys. B **27**, 4391 (1994).
[9] S. Dobosz, M. Lezius, M. Schmidt, P. Meynardier, M. Perdrix, D. Normand, J. P. Rozet, and D. Vernhet, Phys. Rev. A **56**, R2526 (1997).
[10] B. E. Lemoff, G. Y. Yin, C. L. Gordon III, C. P. J. Barty, and S. E. Harris, Phys. Rev. Lett. **74**, 1574 (1995).
[11] T. Ditmire, R. A. Smith, R. J. Marjoribanks, G. Kulcsar, and M. H. R. Hutchinson, Appl. Phys. Lett. **71**, 166 (1997).
[12] T. D. Donnelly, T. Ditmire, K. Neuman, M. D. Perry, and R. W. Falcone, Phys. Rev. Lett. **76**, 2472 (1996).
[13] J. W. G. Tisch, T. Ditmire, D. J. Fraser, N. Hay, M. B. Mason, E. Springate, J. P. Marangos, and M. H. R. Hutchinson, J. Phys. B **30**, L709 (1997).
[14] C. Rose-Petruck, K. J. Schafer, K. R. Wilson, and C. P. J. Barty, Phys. Rev. A **55**, 1182 (1997).
[15] *Molecules and Clusters in Intense Laser Fields*, edited by Jan Posthumus (Cambridge University Press, Cambridge, U.K., 2001), Chaps. 5, 6, and 7.
[16] U. Saalmann and J.-M. Rost, Phys. Rev. Lett. **91**, 223401 (2003); D. Bauer, Laser Part. Beams **21**, 489 (2003).
[17] T. Ditmire, Phys. Rev. A **57**, R4094 (1998).
[18] F. Greschik, L. Dimou, and H.-J. Kull, Laser Part. Beams **18**, 367 (2000).
[19] F. Greschik and H.-J. Kull, Laser Part. Beams **22**, 137 (2004).
[20] D. Bauer, J. Phys. B **37**, 3085 (2004).
[21] P. Mulser, F. Cornolti, and D. Bauer, Phys. Plasmas **5**, 4466 (1998).
[22] T. Ditmire, T. Donnelly, A. M. Rubenchik, R. W. Falcone, and M. D. Perry, Phys. Rev. A **53**, 3379 (1996); B. Shokri, A. R. Niknam and V. Krainov, Laser Part. Beams **22**, 13 (2004).
[23] P. Mulser, H. Takabe, and K. Mima, Z. Naturforsch. A **37**, 208 (1982).
[24] Liu Jiansheng *et al.*, Phys. Rev. A **64**, 033426 (2001).
[25] J. Bréchignac and J. P. Connerade, J. Phys. B **27**, 3795 (1994).
[26] F. Greschik, Ph.D thesis, Rheinisch Westfaelische Technische Hochschule, Aachen, 2002 (unpublished); P. B. Parks, T. E. Cowan, R. B. Stephens, and E. M. Campbell, Phys. Rev. A **63**, 063203 (2001).
[27] P. Mulser, S. Uryupin, R. Sauerbrey, and B. Wellegehausen, Phys. Rev. A **48**, 4547 (1993).
[28] T. Taguchi, Th. M. Antonsen, Jr., and H. M. Milchberg, Phys. Rev. Lett. **92**, 205003 (2004).
[29] Ch. Jungreuthmayer, M. Geissler, J. Zanghellini, and Th. Brabec, Phys. Rev. Lett. **92**, 133401 (2004).
[30] M. Kanapathipillai *et al.*, Phys. Plasmas **11**, 3911 (2004).
[31] S. V. Fomichev, D. F. Zaretsky, and W. Becker, J. Phys. B **37**, L175 (2004).
[32] P. Mulser, F. Cornolti, E. Bésuelle, and R. Schneider, Phys. Rev. E **63**, 016406 (2000).